**SUPPLEMENTARY MATERIAL**

**First chronological constraints for the high terraces of the upper Ebro Catchment**

Parés, J.M., Duval, M., Soria-Jáuregui, A., González Amuchastegui, M.J.
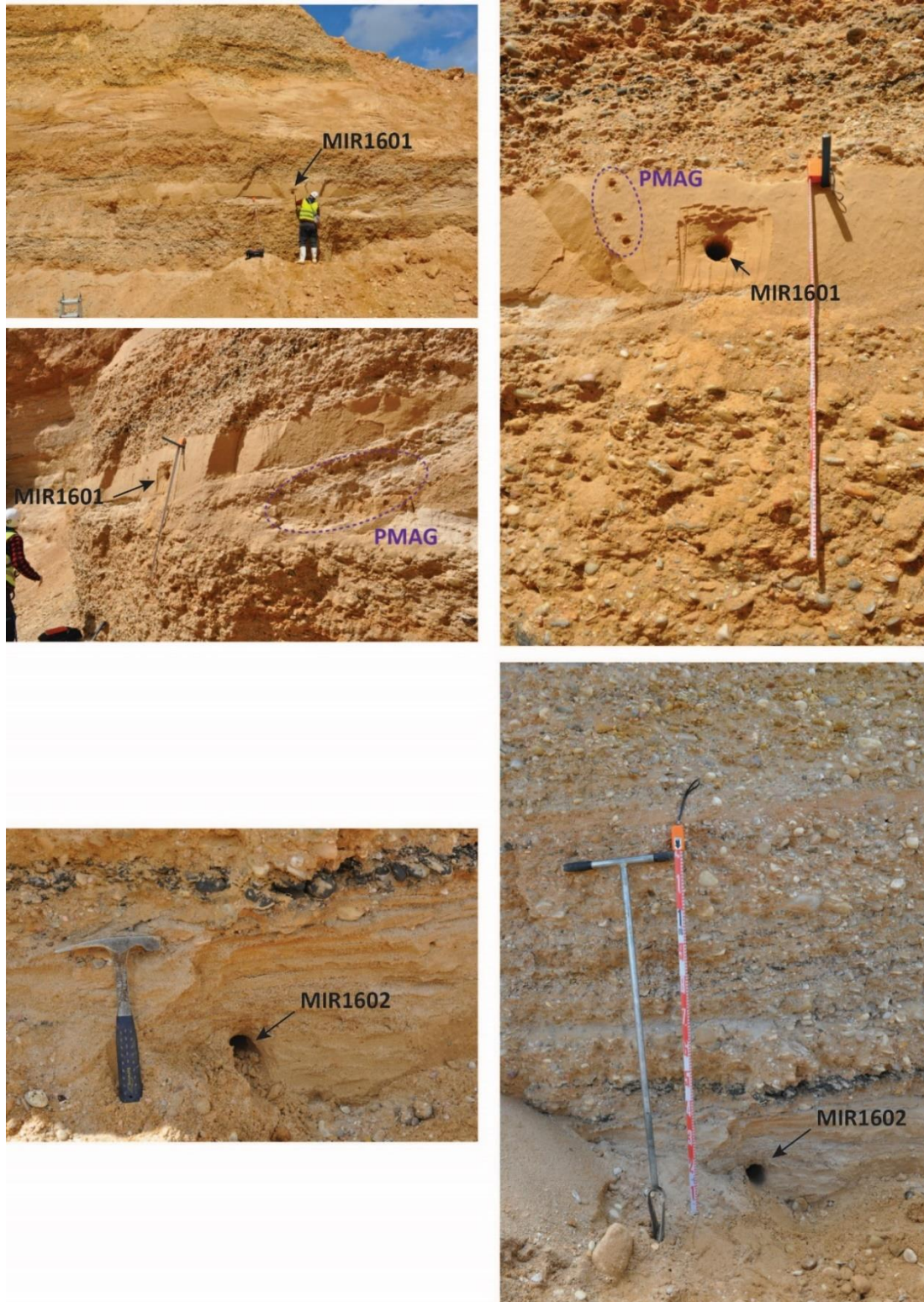
## SM1. ESR and PMAG Sampling

## Figure S1.



*Figure S1: ESR samples MIR1601 and MIR1602, and PMAG samples MIR01 collected from the deposits associated to T1 (+140 m above current river channel).*
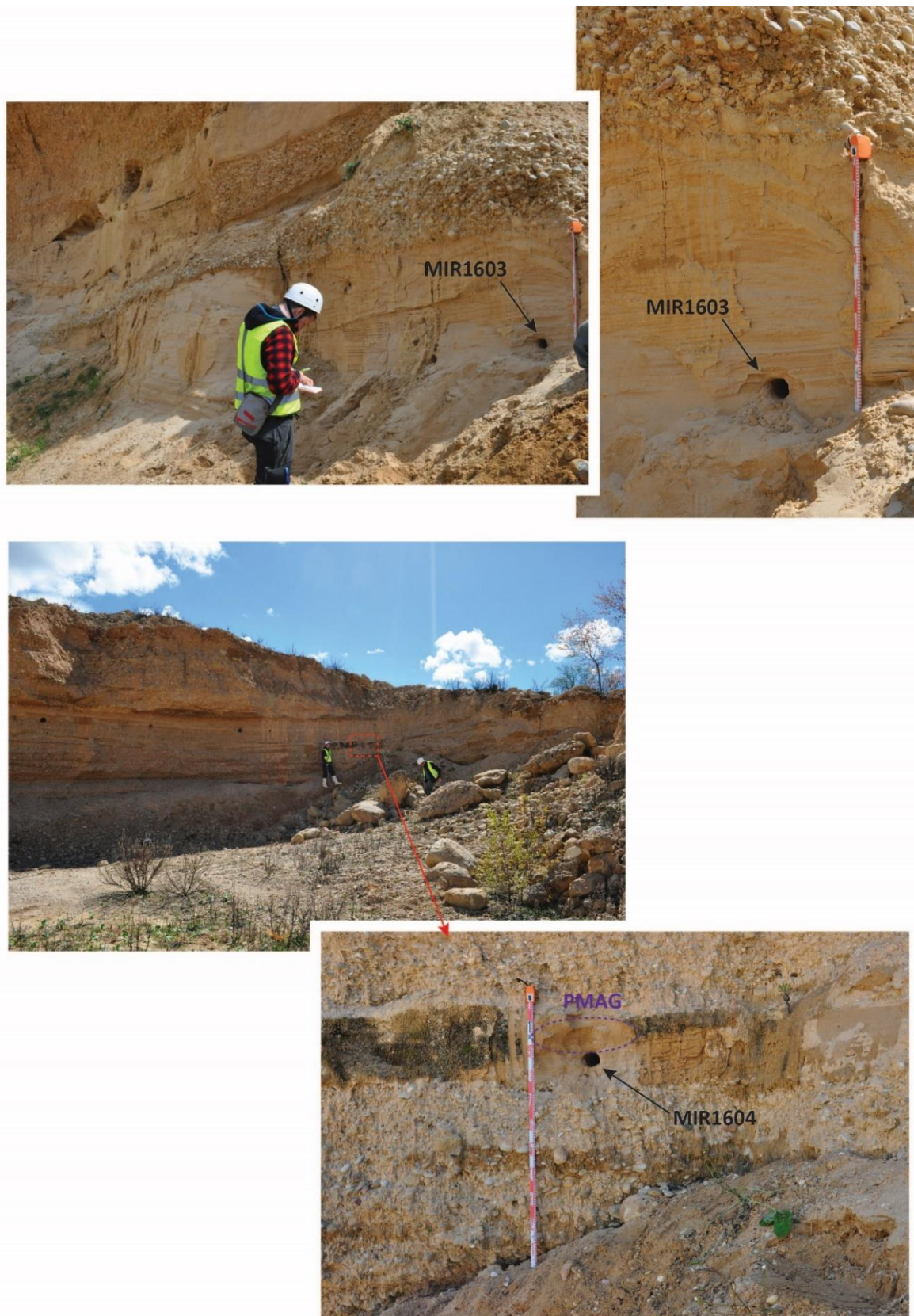
**Figure S2.**



*Figure S2: ESR samples MIR1603 and MIR1604, and PMAG samples MI03 collected from the deposits associated to T2 (+90 m above current river channel).*
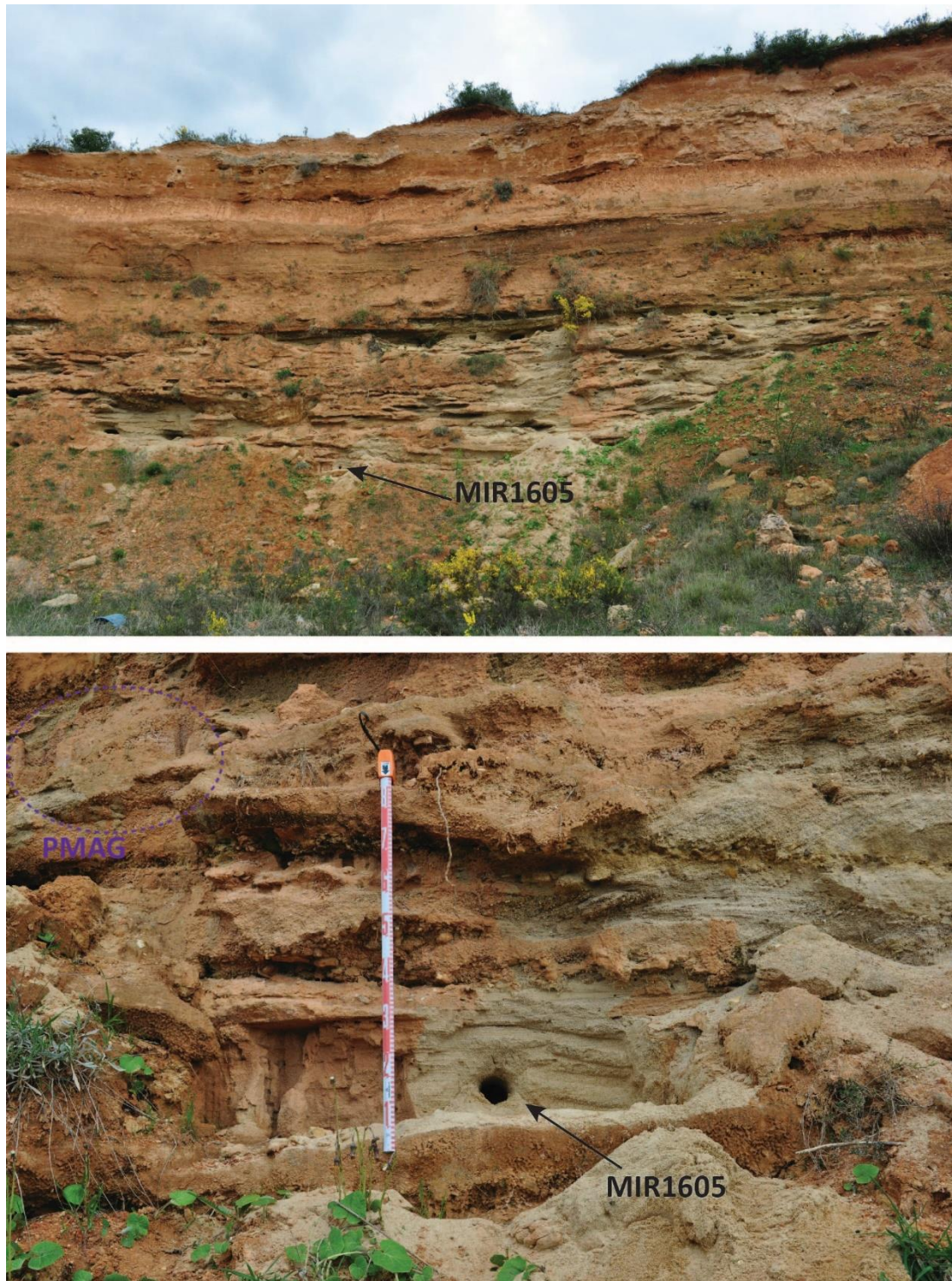
**Figure S3.**



*Figure S3: ESR sample MIR1605 and PMAG sample MI05 collected from the deposits associated to T2 (+85 m above current river channel).*

**SM2. ESR dosimetry**

*Sample preparation*

Sediment samples were prepared in the laboratory under conditions of limited illumination. The 100-200 µm size fraction was collected after wet sieving. HCl (36%) was used to dissolve carbonates and $H_2O_2$ (30%) to eliminate organic matter. Heavy minerals and feldspars were removed with Sodium Polytungstate solutions at d=2.72 and d=2.62 g/ml, respectively. Then, magnetic minerals were eliminated using neodymium magnets. The resulting samples were treated with HF (40%) for 40 minutes to eliminate the remaining feldspars and to etch quartz grains. Finally, HCl (18%) was added in order to remove any soluble fluoride.

*ESR measurements*

Quartz grains were dated by using the Multiple Aliquots Additive Dose (MAAD) method. Each natural sample was divided into 14 aliquots. Twelve aliquots were irradiated using a Gammacell Cs-137 gamma source (dose rate = 6.64 ± 0.15 Gy/min) to the following doses: 100.6, 201.2, 402.6, 805.1, 1610.2, 3220.4, 6038.2, 9057.4, 14089.1, 20127.3, 30191.0, 50318.3 Gy. One of the last two aliquots was kept unirradiated (natural aliquot) while the other one was optically bleached by artificial solar light after exposure in a SOL2 (Dr Hönle) simulator for about 1500 h in order to evaluate the non-bleachable component of the ESR signals associated to the Aluminium (Al) centre.

ESR measurements were carried out at CENIEH (Burgos, Spain), with an EMXmicro 6/1Bruker X-band ESR spectrometer coupled to a standard rectangular ER 4102ST cavity. To ensure constant experimental conditions over time, the temperature of the water circulating in the magnet is controlled and stabilized at 18 ºC by a water-cooled Thermo Scientific NESLAB ThermoFlex 3500 chiller, and the temperature of the room is kept constant at 20 ºC by an air conditioning unit. ESR measurements were performed at low temperature (~90 K) using a ER4141VT Digital Temperature control system based on liquid nitrogen cooling. Further details about the setup and about its stability over time can be found in Duval and Guilarte Moreno (2012) and Duval and Guilarte (2020).

In accordance with the Multiple Centre method defined by Toyoda et al (2000), the ESR signals of both the Al and Ti centers were measured. For the first one, the following acquisition parameters were used: 10 mW microwave power, 1024 points resolution, 20 mT sweep width, 100 kHz modulation frequency, 0.1 mT modulation amplitude, 40 ms conversion time, 10 ms time constant and 1 scan. In contrast, the ESR signal associated to Ti center was measured as

follows: 5 mW microwave power, 1024 points resolution, 20 mT sweep width, 100 kHz modulation frequency, 0.1 mT modulation amplitude, 60 ms conversion time, 10 ms time constant and 1-4 scans depending on the aliquot or sample considered. Each of the thirteen aliquots (one natural, one optically bleached and eleven gamma-irradiated aliquots) of a given sample were measured 3 times after a ~120° rotation in the cavity for both Al and Ti signals in order to consider angular dependence of the signal due to sample heterogeneity. Then, measurements were repeated three to four times over distinct days in order to check the repeatability of the $D_E$ values.

The ESR intensity of the Al signal was extracted from peak-to-peak amplitude measurements between the top of the first peak (g=2.0185) and the bottom of the 16th peak (g=1.9928) (Toyoda and Falguères, 2003). The ESR intensity of the Ti centres has been measured following Duval and Guilarte (2015):

-        Option A: Peak-to-peak amplitude measurement between g=1.979 and the bottom of the peak around g=1.913-1.915, without baseline correction. This intensity most likely results for a mixture of contributions from the Ti-H and Ti-Li centres.

-        Option C: Peak-to-baseline amplitude measurement at g=1.915 without baseline correction. This peak corresponds to a single contribution from the Ti-H centre.

-        Option D: Peak-to-baseline amplitude measurement around g=1.913-1.915 without baseline correction. This peak most likely results for a mixture of contributions from the Ti-H and Ti-Li centres.

-        Option E: Peak-to-baseline amplitude measurement at g=1.979 without baseline correction. This peak corresponds to a single contribution form the Ti-Li centre.

*ESR dose response curve fitting*

For each aliquot, ESR intensities of Al and Ti centres were corrected by the corresponding receiver gain value, number of scans, aliquot mass and a temperature correction factor (Duval and Guilarte Moreno, 2012). The fitting procedures were carried out with the Microcal OriginPro 8.5 software using a Levenberg-Marquardt algorithm by chi-square minimization. Final Dose Response Curves (DRCS) were obtained by pooling the ESR intensities derived from each repeated measurement. For the Al centre, an exponential+linear function (EXP+LIN) was fitted through the experimental points, and data were weighted by the inverse of the squared ESR intensity ($1/I^2$) (Duval, 2012). $D_E$ values were obtained by extrapolating the EXP+LIN function to the residual intensity. For the Ti centres, the function labelled as Ti-

2 in Duval and Guilarte (2015) was used in order to describe the non-monotonic dose dependence of the ESR signal at high doses. Data were weighted by the inverse of the squared experimental error ($1/s^2$) and $D_E$ values were obtained by back extrapolation to Y=0.

## References

Duval, M. (2012). Dose response curve of the ESR signal of the Aluminum center in quartz grains extracted from sediment. Ancient TL 30(2): 1-9.

Duval, M. and Guilarte Moreno, V. (2012). Assessing the influence of the cavity temperature on the ESR signal of the Aluminum center in quartz grains extracted from sediment. Ancient TL 30(2): 11-16.

Duval, M. and Arnold, L.J. (2013). Field gamma dose-rate assessment in natural sedimentary contexts using LaBr3(Ce) and NaI(Tl) probes: A comparison between the "threshold" and "windows" techniques. Applied Radiation and Isotopes 74(0): 36-45.

Duval, M. and Guilarte, V. (2015). ESR dosimetry of optically bleached quartz grains extracted from Plio-Quaternary sediment: Evaluating some key aspects of the ESR signals associated to the Ti-centers. Radiation Measurements 78(0): 28-41.

Guilarte V., Duval M. (2020). ESR dating of optically bleached quartz grains: intra-laboratory comparison of different experimental setups and their impact on dose evaluation. Geochronometria. DOI: 10.2478/geochr-2020-0005.

Toyoda, S. and Falguères, C. (2003). The method to represent the ESR signal intensity of the aluminium hole center in quartz for the purpose of dating. Advances in ESR Applications 20: 7-10.

**Table S1.**

| Sample | Repeated measurements | option A (mixture Ti-Li & Ti-H) | | option E (pure Ti-Li) | |
|---|---|---|---|---|---|
| | | Adjusted $r^2$ | $D_E$ value (Gy) | Adjusted $r^2$ | $D_E$ value (Gy) |
| MIR1601 | 2 | 0.988 | $1073 \pm 61$ | 0.965 | $1209 \pm 115$ |
| MIR1602 | 3 | 0.990 | $949 \pm 46$ | 0.995 | $947 \pm 31$ |
| MIR1603 | 2 | 0.999 | $1135 \pm 34$ | 0.991 | $1331 \pm 54$ |
| MIR1604 | 2 | 0.997 | $1011 \pm 24$ | 0.994 | $1046 \pm 40$ |
| MIR1605 | 3 | 0.994 | $743 \pm 31$ | 0.987 | $870 \pm 38$ |

*Table S1: ESR data derived from the measurement of the Ti centres option A & E* sensu *Duval and Guilarte (2015). Repeatability of the ESR intensities is assessed through the variability (1 relative standard deviation) of the mean ESR intensities obtained after each day of measurements. Similarly, the repeatability of the $D_E$ values corresponds to the variability (1 relative standard deviation) of the $D_E$ values calculated for each day of measurement.*